# PADDY FIELD MAPPING BY INTEGRATING ALOS AVNIR-2 AND PALSAR DATA

Kei Oyoshi and Shinichi Sobue

Earth Observation Research Center, Japan Aerospace Exploration Agency
TSUKUBA SPACE CENTER, 2-1-1 Sengen, Tsukuba, Ibaraki, 305-8505, Japan
Tel: +81-50-3362-7982
E-mail: ohyoshi.kei@jaxa.jp, sobue.shinichi@jaxa.jp

**KEY WORDS** : Food security, Data fusion, Object-based multi-temporal image analysis, Crop phenology

**ABSTRACT** : Food security is one of the critical issues and remote sensing has a large potential to contribute food security through the systematic collection of food security related information such as crop growth or yield estimation. Since Asian countries are responsible for approximately 90% of the world rice production and consumption, rice is the most significant crop, especially in Asia. Accurate paddy field map is imperative to create value-added information about rice in food security. In this research, we mapped paddy field by integrating ALOS AVNIR-2 and PALSAR imagery over Khon Kean, Thailand. PALSAR is useful for paddy field mapping in this region and flooded area can be easily detected by identifying low backscatter coefficient of planting stage. But, PALSAR observes backscatter coefficient of object and the imagery have much speckle noises and heterogeneity. To overcome this problem, we used reflectances of AVNIR-2 for segmentation and derived segments were linked with multi-temporal backscatter of PALSAR. Then, segments of paddy field were detected by using simple thresholding algorithm. Paddy field map derived from Object-based Multi-temporal Image Analysis by integrating AVNIR-2 and PALSAR imagery has less mis-classification due to speckle noise or pixel heterogeneity inherent character of PALSAR data compared to pixel-based classification.

## 1 INTRODUCTION

Food security defined as ”all people, at all times, have physical and economic access to sufficient, safe and nutritious food to meet their dietary needs and food preferences for an active and healthy life” in the World Food Summit of 1996 (World Food Summit, 1996) is a critical issue for the international community, especially in developing countries. In June 2011, the meeting of G20 agriculture ministers was held to improve food security and they agreed on an “Action Plan on food price volatility and agriculture”. In addition to greater and sustainable productivity, this plan emphasis on the better market information that improves transmission of market signals, more open trade, comprehensive rural development and agricultural policies (Meeting of G20 Agriculture Ministers, 2011). Moreover, this plan includes the use of remote sensing tool to improve crop production projections and weather forecasting. Hence, satellite remote sensing is expected to contribute food security through the systematic collection of food security related information such as crop growth or yield estimation. And crop area map is imperative for creating such kind of information.

In Asia, rice is the most significant cereal crop, and Asian countries are responsible for approximately 90% of the world rice production and consumptions. Nevertheless, it is difficult to differentiate paddy field from other crops by remote sensing, because reflectances or backscatters of rice and other crops are quite similar in the vegetated season. In general, paddy field can be detected by using distinctive seasonal characteristic of both flooded and vegetated stages measured by multi-temporal data. Xiao *et al*. (2006) used 8-day MODIS composite data to map continental distribution of paddy field over south and southeast Asia. However, in local scale of paddy field mapping by fine resolution data (less than 100m) with low revisit frequency data, satellite observation by optical sensor in tropics is highly limited by cloud contamination. In contrast, Synthetic Aperture Radar (SAR) can penetrate clouds and collect land-surface information even if the area is covered by cloud. Therefore, SAR sensors onboard airborne or satellite have been used for paddy field mapping. Although the usefulness of SAR imagery for paddy filed have been demonstrated in previous researches (Toan, *et al*, 1989, Zhang, *et al*, 2009), SAR imagery has the problem due to speckle nosies or pixel heterogeneity. Recently, in the crop monitoring with optical imagery, object-based image analysis have been increasingly implemented to overcome pixel heterogeneity (Peña-Barragán *et al*, 2011). This algorithm segments the homogenous land object of the image, after that each segment is classified based on the spectral characteristics of the segment.

In this research, we have implemented object-based image analysis by integrating Advanced Land Observing Satellite (ALOS) Advanced Visible and Near Infrared Radiometer type 2 (AVNIR-2) and Phased Array type L-band Synthetic Aperture Radar (PALSAR) data for paddy field mapping. AVNIR-2 imagery was used for segmentation of land objects in the image and polygon data were created, then multi-temporal backscatter of PALSAR were linked with derived polygons. Finally, paddy filed have been classified based on multi-temporal backscatter of each polygon.

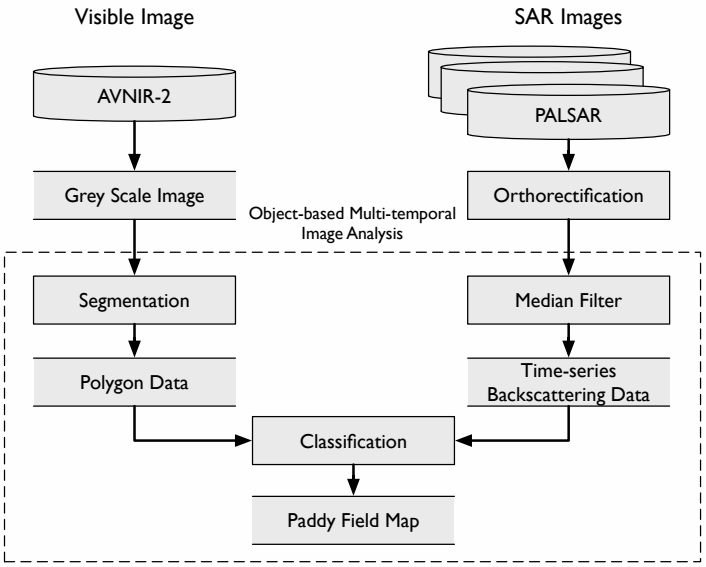


**Figure 1. Framework for paddy field mapping by integrating AVNIR-2 and PALSAR imagery.**

## 2 METHODOLOGY

### 2.1 Study Area and Used Data

Thailand is one of the largest rice production countries and the largest rice exporting country, therefore rice related statistics are imperative for food security and economy in this country. Study area is Khon Kaen (16.455-16.475N, 102.520-102.560E), Thailand located about 400km northeast of Bangkok. In this region, paddy rice is rain-fed cultivation and the yield highly depends on the amount of precipitation. Rice crop is cultivated in May-Oct in rainy season and harvested in Nov-Dec before dry season.

ALOS was launched in January 2006 by Japan Aerospace Exploration Agency and it has been developed to contribute to the fields of mapping, precise regional land coverage observation, disaster monitoring, and resource surveying. It carries three sensors, namely the Panchromatic Remote-sensing Instrument for Stereo Mapping (PRISM), AVNIR-2 and PALSAR. In this study, we used AVNIR-2 imagery to segment landcover objects and multi-temporal PALSAR imagery to characterize crop phenology of segmented objects.

### 2.2 Algorithm for Paddy Detection

Figure 1 shows the framework for paddy field mapping by integrating PALSAR and AVNIR-2 imagery. Basically, paddy field areas were identified by using time-series PLSAR data in flooding and vegetated season. Flooded area is easily detected by PALSAR data, because the backscatter of flooded area shows quite low by specular reflection. Meanwhile, vegetated area has high backscatter because of its volume scattering. However, PALSAR imagery has much speckle noise and the border of each land object is ambiguous compared to that of optical sensor. To overcome this problem, we utilized AVNIR-2 data for segmentation and derived each object was linked with backscattering data of PALSAR. Then, paddy field areas were detected based on multi-temporal backscatter of segmented objects, namely, Object-based Multi-temporal Image Analysis (OMIA).

### 2.3 ALOS Data Processing

Table 1 shows ALOS AVNIR-2 and PALSAR imagery used in this study. Observation mode of PALSAR was Fine Beam Double Polarisation (FBD) mode and HH and HV data were available. The Level1.0 PALSAR data were processed and converted to ortho-rectified data using JAXA/SIG MA-SAR software (Shimada *et al.*, 2010) and SRTM DEM data. Next, backscatter coefficients were calculated by following equation :

$$\sigma^0 = 10 \times \log_{10}[DN]^2 - 83.0 \,, \tag{1}$$

**Table 1. Specifications of ALOS AVNIR-2 and PALSAR imagery in this study.**

| | AVNIR-2 | PALSAR |
|---|---|---|
| Spatial Resolution | 10.0m | 12.5m |
| Band | 4-band (RGB and NIR) | L-band (1.27GHz) |
| Polarization | - | HH and HV |
| Incidence Angle | - | 34.3 deg. |
| Observed Date | 2008/04/26 | 2008/06/03 |
| | | 2008/07/19 |
| | | 2008/09/13 |
| | | 2008/10/19 |

where, $\sigma^0$ means backscatter coefficient ($dB$), $DN$ is digital number of PALSAR data. Then, median filter with 3×3 pixels were applied to reduce speckle noises. These multi-temporal backscatter data were utilized to characterize the phenology of paddy field.

For segmentation processing, AVNIR-2 Level1B2 RGB and NIR bands were used. First, these images were normalized to the brightness distribution whose mean and standard deviation were 320 and 80, respectively. These images were converted to gray scale image by simply calculating their average, then gray scale image was also normalized to the brightness distribution whose mean and standard deviation were 320 and 80, respectively. Gray scale image was segmented into multi-pixel objects by using iterative region growing algorithm (Tomita *et al.*, 1982). This algorithm merge into adjacent pixels whose gray level difference is less than the threshold, and the gray level of each region is averaged. Then, threshold is increased and the merging process is repeated. In this study, we experimentally determined the number of iterations (five times) and threshold of 3, 6, 9, 12, 15. By this processing, segmented image of land objects were created.

Derived segmented image were overlaid with PALSAR imagery, and backscatter of each segment were calculated by averaging backscatter of corresponding pixels in PALSAR imagery. These object-based multi-temporal backscatter data were used for Object-based Multi-temporal Image Analysis to detect paddy field.

## 3 RESULTS AND DISCUSSIONS

### 3.1 Segmentation by AVNIR-2 Data

Figure 2 illustrates the segmented images of AVNIR-2 imagery by iterative region growing algorithm. Constructed segments agree with land objects by visual interpretation of true color image of AVNIR-2. However, some land objects were difficult to merge into one segment, for example, grey level in urban area is highly variable because of its heterogeneity. Further researches on segmentation including algorithm or determination of threshold are imperative to improve the accuracy of segmentation. Moreover, although proposed methodology uses AVNIR-2 image acquired on 26 Apr 2008 for segmentation, we have to select a proper image in terms of not only cloud coverage, but also observational date to maximize the segmentation accuracy.

### 3.2 Seasonal Variations in PALSAR Backscattering Coefficients

Seasonal changes in PALSAR backscattering coefficient (HH and HV polarization) of five landcover types (paddy, forest, urban, water) are shown in Figure 3. Sample data (average of each polygon) were selected based on visual interpretation of AVNIR-2 imagery. Backscatter of forest or urban areas were higher than other landcover because their surfaces are rough in terms of PALSAR wavelength and cause volume scattering. On the other hand, backscatter of water body indicated lower because of specular reflection. In this region, rain-fed rice are planted in May-Jun and harvested in Nov-Dec. Since paddy field has flooding and vegetated stages, we assume that backscatter of paddy field increase in this period (Jun-Oct). Actually, HH and HV backscatter of paddy field are increase. In addition, HH of paddy field are higher than that of HV, and also the variation width of HH is larger than that of HV. This is consistent with the result of ground-based measurements of L-band full-polarization backscatter over paddy field (Inoue *et al*, 2002). Hence, separability of paddy field from other landcover by using HH polarization is higher than by using HV polarization and we utilized HH data for paddy field detection. In this study, segmented objects whose seasonal variations of HV polarization intersect -12.5 dB were classified into paddy field.

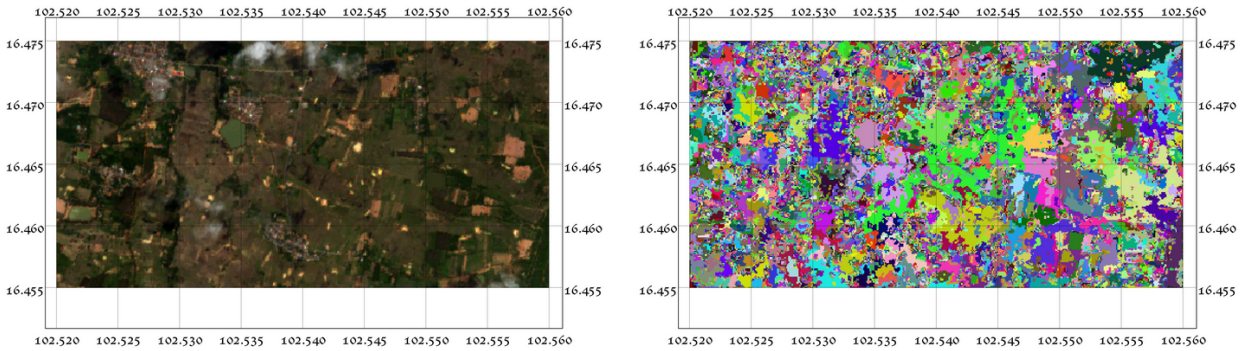


(a) True color image (b) Segmented image

**Figure 2. True color and segmented images of AVNIR-2 data over study area, Khon Kaen in Thailand.**

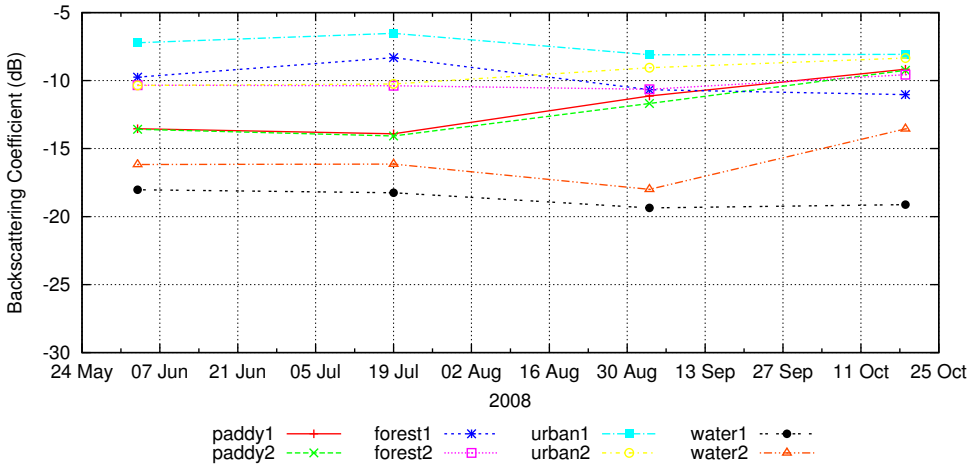


(a) HH polarization

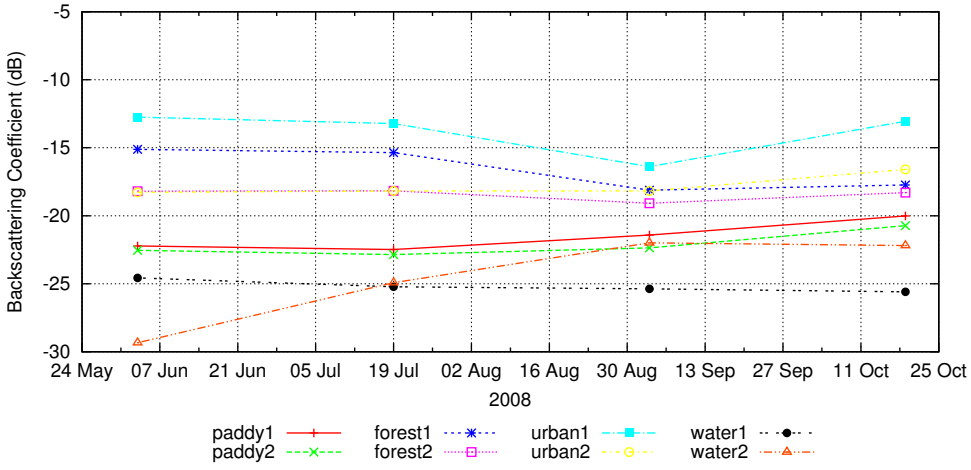


(b) HV polarization

**Figure 3. Seasonal changes of HH and HV backscattering over four landcover.**

### 3.3 Result of Paddy Field Detection

By integrating AVNIR-2 and PALSAR imagery, object-based multi-temporal image analysis was implemented to detect paddy field area. Figure 4 illustrates the comparison of paddy field map derived from pixel-based and object-based algorithm. Both map were created by using same threshold to detect paddy field area. The result of pixel-based classification (Figure 4-a) has a lot of small patches result from speckle noise. There are small patches of commission error in forest or urban area and omission error in paddy field area by visual interpretation. In contrast, the paddy field map derived from object-based classification have few small patches and detected areas are well aggregated. Further validation with ground truth data is necessary to assess the accuracy of the paddy field map derived from object-based multi-temporal image classification.

In this study, the classification algorithm was simple thresholding method and this may caused mis-classification. To improve the accuracy of paddy field detection, statistical algorithm with validation data should be considered. However, proposed framework by integrating AVNIR-2 and PALSAR imagery worked better and the accuracy of derived map is better than that of pixel based map based on the visual interpretation. In addition, proposed methodology of automatic creation of polygon data from AVNIR-2 is cost-effective. This is absolutely imperative for practical use for paddy mapping, because in general, creating polygon data is time and cost consuming work.

## 4 CONCLUSIONS

We have developed the algorithm for paddy field mapping by integrating AVNIR-2 and PALSAR data with object-based multi-temporal image analysis. This study demonstrated the advantage of combining optical data for segmentation and microwave data for characterizing crop phenology over tropics highly clouded area. Proposed methodology is able to reduce mis-classification due to speckle noise or pixel heterogeneity inherent character of PALSAR data. However, in order to improve the accuracy of paddy field detection, the algorithm for segmentation or classification should be modified. Also, further validation is need to assess applicability for other areas.

## REFERENCES


[1] World Food Summit Plan of Action. World Food Summit, Rome, Italy, Nov. 1996.

[2] Action plan on food price volatility and agriculture. Meeting of G20 Agriculture Ministers, Paris, France, Jun. 2011.

[3] Xiao, X., Boles, S., Frolking, S., Li, C., Babu, J. Y., Salas, W. and Moore III, B., 2006. Mapping paddy rice agriculture in South and Southeast Asia using multi-temporal MODIS images. Remote Sensing of Environment, 100, pp.95-113.

[4] Toan, T. L.. Laur, H., Mougin, E., and Lopes, A., 1989. Mapping paddy rice agriculture in South and Southeast Asia using multi-temporal MODIS images. IEEE Transactions of Geoscience and Remote Sensing, 27(6), pp.709-718

[5] Zhang, Y., Wang, C., Wu, J., Qi, J. and Salas, W. A., 2009. Mapping paddy rice with multitemporal ALOS/PALSAR imagery in southeast China. International Journal of Remote Sensing, 30(23), pp.6301-6315.

[6] Peña-Barragán, J. M., Ngugi, M. K., Plant, R. E. and Six J., 2011. Object-based crop identification using multiple vegetation index, textural features and crop phenology. Remote Sensing of Environment, 115, pp.1301-1316.

[7] M. Shimada, 2010. Ortho-rectification and Slope Correction of SAR Data Using DEM and Its Accuracy Evaluation,IEEE Journal of Selected Topics in Applied Earth Observations and Remote Sensing, 3(4), pp.657-671.

[8] Tomita, F.,Shirai, Y., and TSUJI, S.,1989. Description of Texture by a Structural Analysis. IEEE Transactions of Pattern Analysis and Machine Inteligence, 4(2), pp.183-191

[9] Inoue, Y., Kurosu, T., Maeno, H., Uratsuka, S., Kozu, T., Dabrowska-Zielinska, K. and Qi, J, 2002. Season-long daily measurements of multifrequency (Ka, Ku, X, C, and L) and full-polarization backscatter signatures over paddy rice field and their relationship with biological variables. Remote Sensing of Environment, 81, pp.194-204.

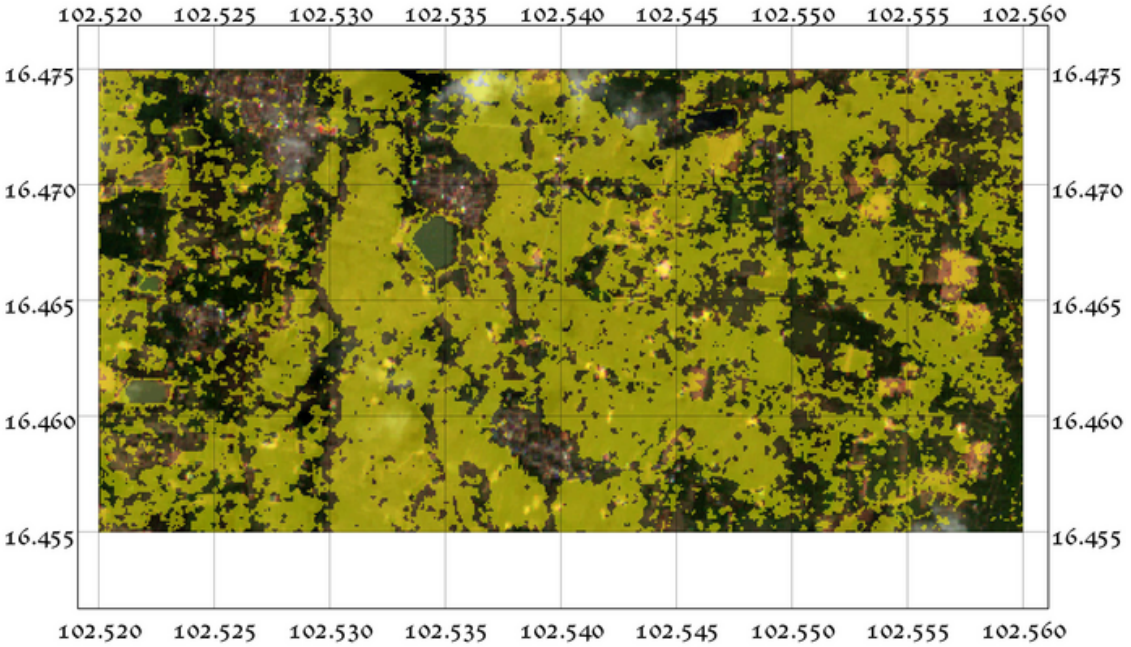


(a) Pixel-based classification

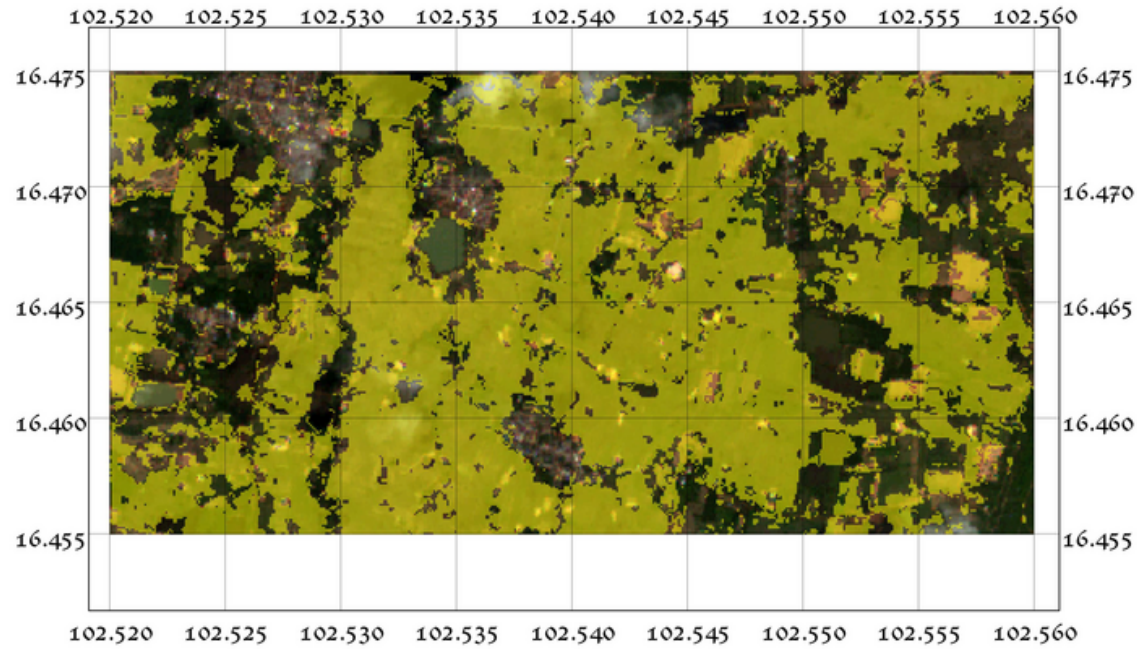


(b) Object-based classification

**Figure 4. Comparison of detected paddy field maps. Yellow color means paddy field.**